IEEE Access
Multidisciplinary ⋮ Rapid Review ⋮ Open Access Journal

Received 12 February 2024, accepted 4 March 2024, date of publication 7 March 2024, date of current version 13 March 2024.

Digital Object Identifier 10.1109/ACCESS.2024.3374333

RESEARCH ARTICLE

Fully Tunable Bandpass Filter With Wide Bandwidth Tuning Range and Switchable Single/Dual Band

SHUANG LI, SHENGXIAN LI, JIANRONG YUAN, JUN LIU, AND MAN SHI
China Academy of Space Technology (Xi'an), Xi'an 710100, China
Corresponding author: Shuang Li (lishuang8118@163.com)

ABSTRACT In this paper, a fully tunable bandpass filter (BPF) with three states of filtering (single passband state, dual passband state and all-off state) is proposed, the proposed fully tunable BPF is cascaded by a tunable low pass filter section (LP) and a tunable high pass filter section(HP). By introducing a switchable dual-mode notch in the passband, the proposed BPF is capable of operating in single, dual passband and all-off state, demonstrating high flexibility in working mode. Tunable LP and HP filters with 7-order generalized Chebyshev response are designed to improve the roll-off rate and out-of-band rejection level of the BPF. The measured results show that the bandwidth of the BPF can be tuned from 0.25GHz to 2.69GHz (10.8:1), and the center frequency can be tuned from 2.9GHz to 4.6GHz with constant absolute bandwidth of 1GHz. Besides, high rejection level of out-of-band is realized in all working mode. The high flexibility in working mode makes the proposed fully tunable BPF very attractive in carrier aggregation scenarios.

INDEX TERMS High pass filter, low pass filter, switchable single and dual band, tunable bandpass filter, varactor and PIN diode.

I. INTRODUCTION

With the development of modern wireless communication systems, more frequency bands are utilized and RF front-ends need to operate at multiple frequency bands [1]. The traditional RF front-end solution termed filter bank to achieve multi-band compatibility generally occupy large area on circuit board and have high costs [2]. The tunable bandpass filters which can support numerous frequency bands with a single filter structure may meet the requirements of miniaturization, integration and low cost, is one of the promising microwave components for future wireless communications [3].

Recently, fully tunable BPFs with frequency and bandwidth tunable have attracted much attention due to their high flexibility. Numbers of fully tunable BPFs have been proposed and these fully tunable BPFs can be divided into three categories according to the tuning mechanism. The first class of fully tunable BPFs based on multimode resonators (MMRs) is proposed in [4], [5], [6], and [7]. In [4], a wideband fully tunable bandpass filter with three adjustable poles is proposed, and the three adjustable poles are generated by MMRs and can be adjusted independently, as a result, the tunable frequency and bandwidth can be achieved by controlling the independent poles. In [5], a fully tunable BPF based on spilt-ring resonator with three short-stub tapped is presented, and the proposed filter can realized operational agility of the center frequency and bandwidth. In [7], the fully tunable BPF comprises a multi-resonant cell and two quarter-wavelength coupled line resonators and exhibits a three-pole/two transmission zero response. The tunability of frequency and bandwidth can be achieved by solely reconfiguring the resonant frequency of its constituent resonators. Besides, the proposed BPF based on multilayer integration concept owns compact size. The second class of fully tunable BPFs based on coupled resonators is proposed in [8], [9], [10], [11], [12], [13], [14], [15], and [16]. In [8], a two-pole tunable combline filter that allows for operational agility

The associate editor coordinating the review of this manuscript and approving it for publication was Feng Lin.

of the center frequency, passband bandwidth is proposed, a pair of varactor diodes is added between the resonators to adjust the coupling coefficient, so the bandwidth of the filter can be tuned. In order to enhance the frequency tuning range, a compact switchable and fully tunable BPF is presented in [11]. The selectivity of the two-pole filter is poor. To improve the selectivity of fully tunable filters, a 5-order fully tunable filter is demonstrated in [14], the bandwidth of the filter can be varied by controlling the varactors between resonators. Nevertheless, these fully tunable BPF based on coupled resonators cannot achieve wide bandwidth tuning range due to the limitation of coupling coefficient. The third class of fully tunable BPFs realized by cascading tunable LPF and HPF is proposed in [17], [18], and [19]. However, the performance of the proposed filters in [17], [18], and [19] such as bandwidth tuning ranging and rejection level of stopband should be improved. Thus, it is still a challenge to design a fully tunable filter with good performance such as bandwidth tuning range and rejection level of stopband.

In this paper, a fully tunable BPF with wide bandwidth tuning range and switchable single/dual band is proposed, the proposed filter is cascaded by a tunable LPF, a tunable HPF and a switchable notch filter. The flexible frequency and bandwidth of the filter are realized by changing the cutting-off frequency of the tunable LPF and HPF. To improve the performance of the BPF, a tunable 7-order quasi-ellipse LPF and HPF are designed. Besides, the filter can achieve a single or dual passband state by controlling the ON/OFF state of the switchable notch filter. For validation, the proposed filter is fabricated and measured. The proposed filter exhibits high flexibility and is very attractive in carrier aggregation scenarios.

II. DESIGN OF FULLY TUNABLE BANDPASS FILTER

The proposed fully tunable BPF with wide bandwidth tuning range and switchable single/dual band consists of three parts, i.e. tunable LPF, HPF and switchable notch filter. In this section, firstly, the analysis of schematic structure of the proposed BPF is presented using the scattering matrix, then detailed design process of the three parts is given. Lastly, the design of the proposed BPF is provided.

A. SCHEMATIC ANALYSIS

The proposed fully tunable BPF is cascaded by tunable LPF, HPF and switchable notch filter, as shown in Fig. 1.

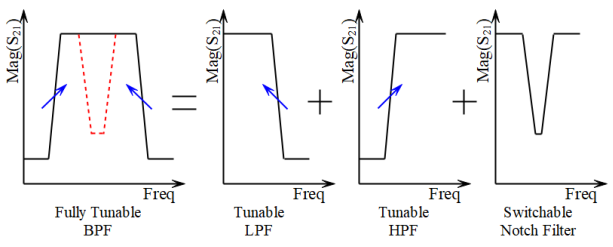

FIGURE 1. Schematic of the proposed filter.

The S parameter of the proposed schematic is shown in Fig. 2. S_L, S_H and S_N represent the scattering matrix of the tunable LPF, HPF and switchable notch filter, respectively. V_1^+, V_2^+, V_3^+ and V_4^+ denote the voltage incident wave of the cascading network., while the voltage reflected wave are denoted by V_1^-, V_2^-, V_3^- and V_4^-.

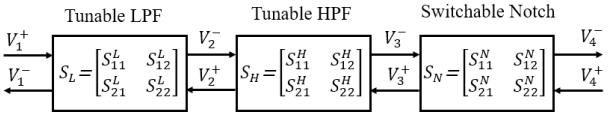

FIGURE 2. Scattering parameter of the proposed schematic.

Using the scattering matrixes of the bifurcation networks, the relationships between the voltage incident and reflected waves defined at their ports can be obtained as Equations (1)-(3).

$$\begin{bmatrix} V_1^- \\ V_2^- \end{bmatrix} = \begin{bmatrix} S_{11}^L & S_{12}^L \\ S_{21}^L & S_{22}^L \end{bmatrix} \begin{bmatrix} V_1^+ \\ V_2^+ \end{bmatrix} \tag{1}$$

$$\begin{bmatrix} V_2^+ \\ V_3^- \end{bmatrix} = \begin{bmatrix} S_{11}^H & S_{12}^H \\ S_{21}^H & S_{22}^H \end{bmatrix} \begin{bmatrix} V_2^- \\ V_3^+ \end{bmatrix} \tag{2}$$

$$\begin{bmatrix} V_3^+ \\ V_4^- \end{bmatrix} = \begin{bmatrix} S_{11}^N & S_{12}^N \\ S_{21}^N & S_{22}^N \end{bmatrix} \begin{bmatrix} V_3^- \\ V_4^+ \end{bmatrix} \tag{3}$$

From (1)-(3), the voltage reflected wave can be obtained as Equation (4)-(6).

$$V_2^- = S_{21}^L V_1^+ + S_{22}^L V_2^+ \tag{4}$$

$$V_3^- = S_{21}^H V_2^- + S_{22}^H V_3^+ \tag{5}$$

$$V_4^- = S_{21}^N V_3^- + S_{22}^N V_4^+ \tag{6}$$

It is assumed that the tunable LPF, HPF and notch filter realize ideal impedance match with each other, that means,

$$V_2^+ = V_3^+ = 0 \tag{7}$$

Hence, the voltage transmission coefficient of the entire topology are,

$$S_{21,total} = \frac{V_4^-}{V_1^+}|_{V_4^+=0} = S_{21}^L S_{21}^H S_{21}^N \tag{8}$$

From Equation (8), it can be concluded that the voltage transmission coefficient of the fully tunable BPF is the product of the voltage transmission coefficient of the tunable LPF, HPF and switchable notch filter, therefore, a BPF with switchable single/dual band can be realized by cascading a LPF, HPF and switchable notch filter directly.

B. DESIGN OF SWITCHABLE NOTCH FILTER

In this section, detailed theoretical analysis and design process of the switchable notch filter are given. The proposed topology structure of notch filter is shown in Fig. 3(a). The filter is composed of two identical series resonators, which are connected by a transmission line with an electrical length

of 90° and a characteristic impedance of Z_T. To expand the bandwidth of the notch band, capacitive coupling denoted by C_M between the two series resonators are introduced.

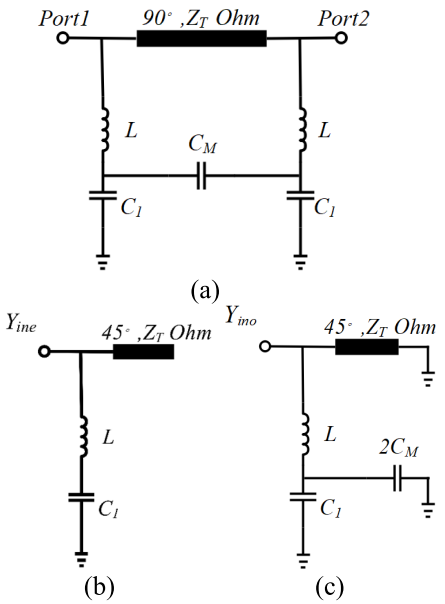

FIGURE 3. (a) Topology of notch filter (b) Even-mode equivalent circuit (c) Odd-mode equivalent circuit.

The even- and odd-mode equivalent circuits of the notch filter are shown in Fig. 3(b) and 3(c), respectively. The input admittance of even-mode and odd-mode can be calculated by Equation (9) and (10). According to the resonance condition $\mathrm{Im}(Y_{in}) = 0$, even-mode and odd-mode resonance frequency of notch filter can be obtained. As shown in Equation (9) and (10), the even-mode resonance frequency is determined by L and C_1, while the odd-mode resonance frequency is also affected by coupling capacitor C_M, thus, by adjusting the coupling C_M, the bandwidth of notch band can be tuned.

$$Y_{ine} = \frac{1}{\left(j\omega L + {}^{1}\!/_{j\omega C_1}\right)} + \frac{j}{Z_T} \tag{9}$$

$$Y_{ino} = \frac{1}{\left(j\omega L + {}^{1}\!/_{j\omega (C_1 + 2C_M)}\right)} + \frac{1}{(jZ_T)} \tag{10}$$

The L, C_1, C_M and Z_T values in Fig. 3(a) can be synthesized based on the method introduced in [17], using the Equations (11)-(15), where g_0–g_3 are the element values of the low-pass filter prototype, ω_0 is the central frequency of the filter, Z_0 is the port impedance, and FBW is the fractional bandwidth, k is the coupling coefficient between the two resonators.

$$Z_T = \frac{Z_0}{\sqrt{g_0 g_3}} \tag{11}$$

$$L = \frac{Z_0}{\omega_0 \sqrt{g_1 g_2} \cdot \mathrm{FBW}} \tag{12}$$

$$C = \frac{1}{\omega_0^2 L} \tag{13}$$

$$C_M = \mathrm{FBW} \cdot kC \tag{14}$$

$$C_1 = C - C_M \tag{15}$$

The coupling coefficient k is proportional to the coupling C_M. As shown in Fig. 4, when the coupling coefficient k is increased, the bandwidth of the notch filter is widen, however, the rejection level of notch band deteriorates, simultaneously. Therefore, k can be determined based on the required the bandwidth of the notch band.

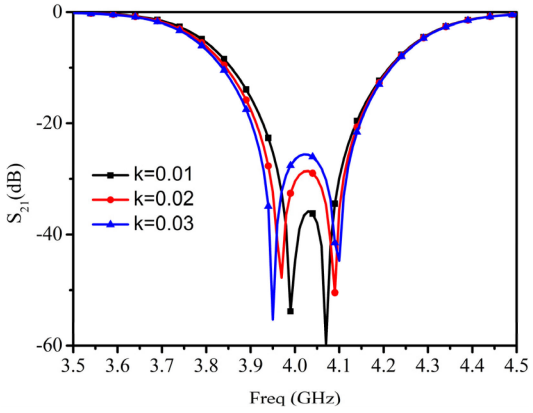

FIGURE 4. S_{21} of notch filter with different coupling coefficient k.

The inductors and capacitors can be realized by high- and low-impedance stubs, respectively. The dimensions of stubs can be calculated by Equation (16) and (17), where ω_c and λ_g denote the cut-off frequency of the filter and corresponding wavelength in substrate, l and Z_0 denote the physical length and characteristic impedance of the stubs, and L and C are the values of inductor and capacitor in topology.

$$l = \frac{\lambda_g}{2\pi} \arcsin(\omega_C L / Z_0) \tag{16}$$

$$l = \frac{\lambda_g}{2\pi} \arcsin(\omega_C C Z_0) \tag{17}$$

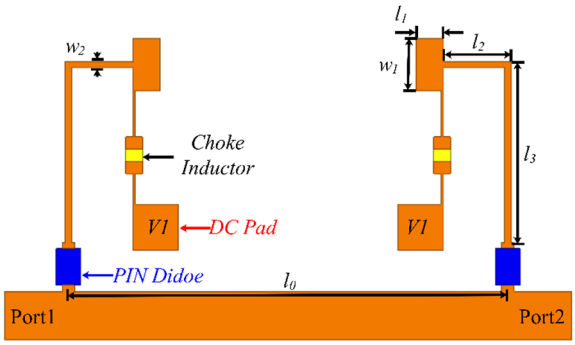

FIGURE 5. Layout of the proposed notch filter.

The layout of the proposed switchable notch filter is shown in Fig. 5. The capacitor and inductor are realized by stubs with width w_1 and w_2, respectively. To achieve coupling C_M, the two low-impedance stubs bend toward the middle of

the filter. To realize switchable characteristic, two PIN diodes are used to connect series resonators and transmission line, the ON/OFF state of PIN diode can be controlled by the voltage V1 applied to the DC pads, and the bias network is connected with the notch filter using 470 nH choke inductors, and the choke inductors exhibit high impedance characteristics, so the bias network has less effect on the filter. PIN diode SMP1345 from Skyworks is chosen to control the notch band.

The notch filter is designed on Rogers 5880 with relative dielectric constant $\varepsilon_r = 2.2$ and thickness $h = 0.508$ mm. The filter is optimized by HFSS, and the final dimensions are as follows, $l_0 = 14.4$ mm, $l_1 = 0.9$ mm, $l_2 = 2.2$ mm, $l_3 = 5.9$ mm, $w_1 = 2$ mm, $w_2 = 0.2$ mm.

The simulated result of the proposed switchable notch filter is shown in Fig. 6. When the PIN diode is in OFF state, the notch filter is equivalent to quarter wavelength transmission line, and exhibits all-pass characteristic. When the PIN diode is in ON state, the notch filter is a dual-mode bandstop filer, the center frequency of the notch band is 3.8 GHz, and the 2 dB notch bandwidth is 420 MHz(3.57-3.99 GHz).

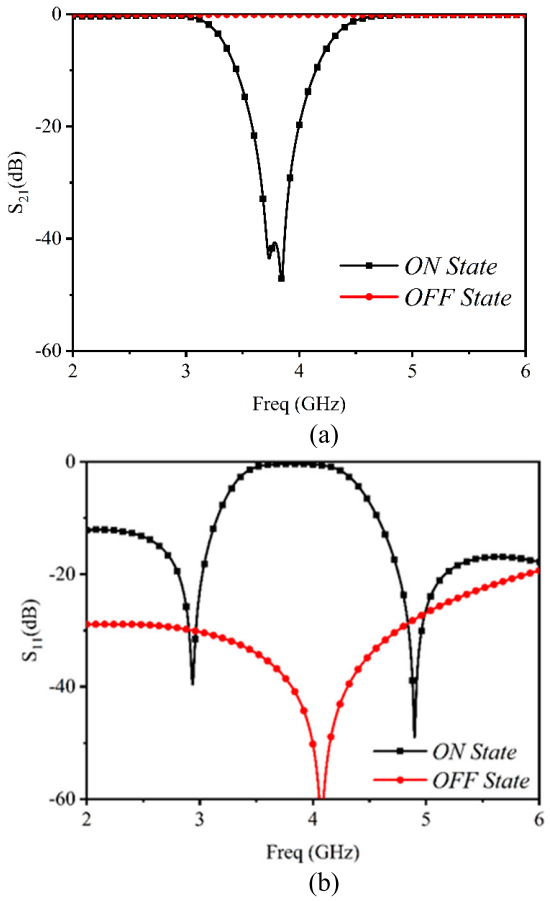

FIGURE 6. Simulated result of the switchable notch filter (a) S_{21} (b) S_{11}.

C. DESIGN OF TUNABLE LPF

In order to improve the out-of-band rejection level, a 7-order tunable LPF with quasi-ellipse response is proposed. Compared with the Butterworth or Chebyshev response filter, the proposed filter can generate a transmission zero in the stopband, which can enhance the selectivity and out-of-band rejection level of the filter. The topology structure of the proposed tunable LPF is shown in Fig. 7, the capacitors in series resonators are replaced with varactor diodes, thus cut-off frequency of the LPF can be tunable by controlling the bias voltage of the varactors C_{v1} and C_{v2}.

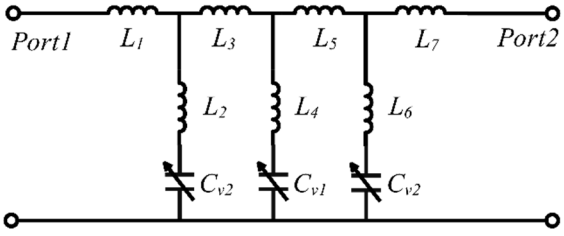

FIGURE 7. Topology of the tunable LPF.

The inductance $L_1 \sim L_7$ can be realized by high-impedance stubs. The element values in the topology can be synthesized easily by using the method introduced in [18]. The physical dimensions of the high-impedance stubs can be obtained by Equation (16).

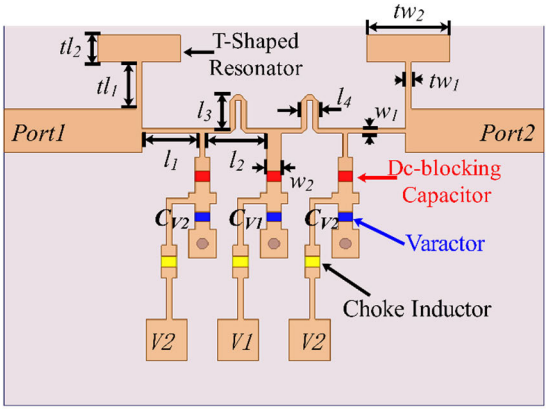

FIGURE 8. Layout of the tunable LPF.

The layout of the proposed LPF is shown in Fig. 8. The filter is also designed on Rogers 5880. The commercial varactor diode SMV1430 from Skyworks is chosen as the tuning element with a tuning range from 0.31 pF (30 V) to 1.24 pF (0 V). The effective capacitance of the varactors can be adjusted by DC voltage *V1* and *V2*. The DC bias lines are connected to filter by 470 nH choke inductors to reduce the influence on LPF. DC-blocking capacitors with value of 3 pF are used to separate bias circuit and filter.

To improve the rejection level of stopband furtherly, T-shaped resonators are introduced to generate a transmission zero. Fig. 9 shows the transmission coefficient S_{21} of the LPF. As shown in Fig. 9, a transmission zero at about 9GHz is produced, and the rejection level of stopband is enhanced significantly, while the passband changed slightly.

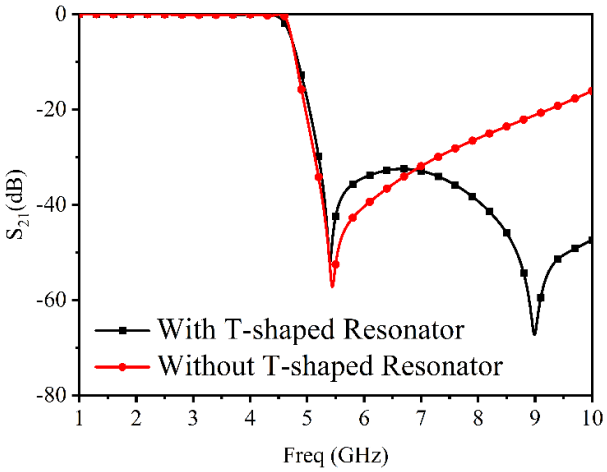

FIGURE 9. Transmission coefficient S21 of the tunable LPF.

The EM simulation software HFSS is utilized to optimize the proposed filter. And the final dimensions are listed as follow: $l_1 = 2.1$ mm, $l_2 = 1.78$ mm, $l_3 = 1.22$ mm, $l_4 = 0.6$ mm, $w_1 = 0.2$ mm, $w_2 = 0.43$ mm, $tl_1 = 1.72$ mm, $tl_2 = 1.14$ mm, $tw_1 = 0.2$ mm, $tw_2 = 3$ mm. The simulated results of the tunable LPF are shown in Fig. 10. As shown, the cut-off frequency of the proposed LPF can be tuned from 3.4 GHz to 5.2 GHz. During the whole tuning range, the in-band return loss is greater 12.5 dB, and the rejection level of stopband is greater than 30 dB.

D. DESIGN OF TUNABLE HPF

A 7-order tunable HPF with quasi-ellipse response is proposed in this section. The topology of the proposed tunable HPF is shown in Fig. 11. A transmission zero in the stopband can be generated due to the two series resonators, thus the rejection level of the stopband is enhanced.

The capacitors C_3 and C_5 in series resonators are replaced by varactor diodes, thus the cut-off frequency of the HPF can be varied by tuning the bias voltage of varactors.

The capacitor C_4 in the topology is also replaced by varactor diode to compensate the impedance mismatch during the tuning process. As shown in Fig. 12, the curve in black color is the original state of the tunable HPF. The cut-off frequency of HPF can be tuned to a lower frequency as shown in red color by changing the bias voltage of varactor C_3, C_5 and keeping C_4 unchanged. However, the in-band return loss of HPF deteriorates during the tuning process. When changing C_3, C_4 and C_5 simultaneously, the S_{11} of the tunable HPF is improved as shown in blue color.

The cut off frequency of filter changes slightly by tuning the capacitors C_2 and C_6 in the topology, thus the capacitors C_2 and C_6 are realized by interdigital structure instead of varactor diodes, besides, the interdigital structure can also significantly simplify the design of varactor bias circuit.

The layout of the proposed tunable HPF is shown in Fig. 13. The capacitors C_3 and C_5 in topology are realized

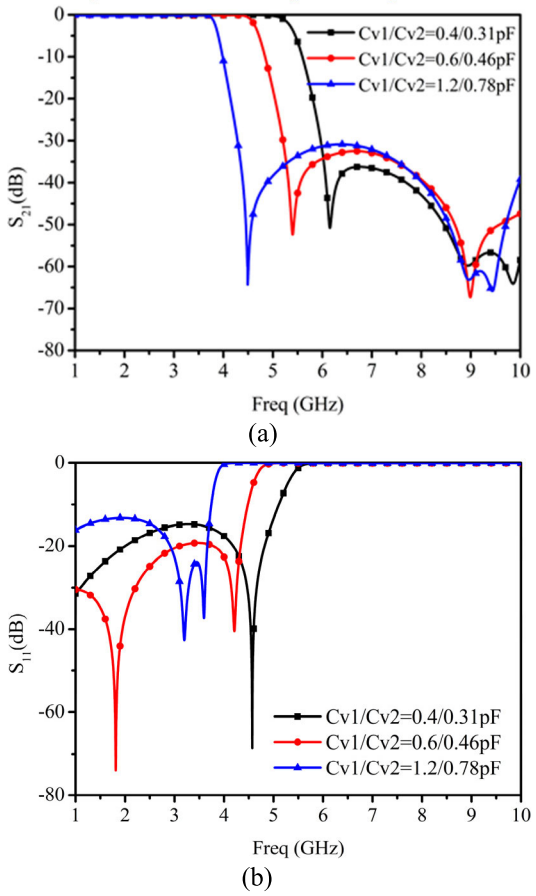

FIGURE 10. Simulated results of tunable LPF (a) S_{21} (b) S_{11}.

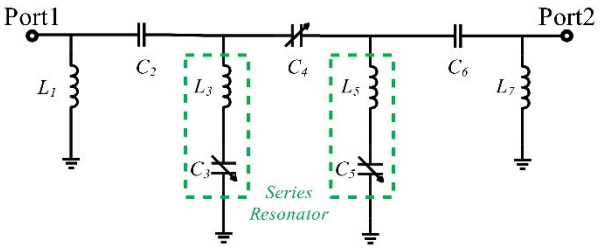

FIGURE 11. Topology of the tunable HPF.

by varactor C_{v1}, while the capacitor C_4 is realized by a common-cathode varactor pair C_{v2}, and the efficient capacitance of C_{v1} and C_{v2} can be controlled by changing the bias voltage V1 and V2. The biasing network is connect to the filter through 470nH inductors. And varactors SMV1408 and SMV1405 are chosen to realize C_{v1} and C_{v2}, respectively. The inductors L_1, L_3, L_5 and L_7 in topology are realized by high-impedance stubs, and the physical dimensions can be obtained by Equation (16).

The tunable HPF is also designed on Rogers 5880. After optimization by HFSS, the final dimensions of the HPF are as follows, $l_1 = 4.4$ mm, $l_3 = 3.6$ mm, $w_1 = 0.5$ mm, $w_2 = 1.05$ mm, $zl = 3.6$ mm, $zw = 0.2$ mm, $zs = 0.1$ mm. The overall filter dimension is 21.1 mm × 6.5 mm.

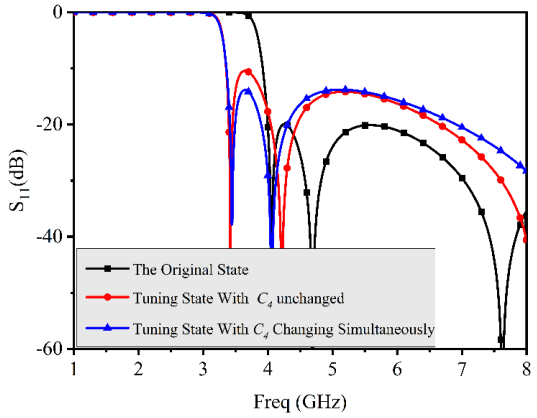

FIGURE 12. S_{11} of the tunable HPF.

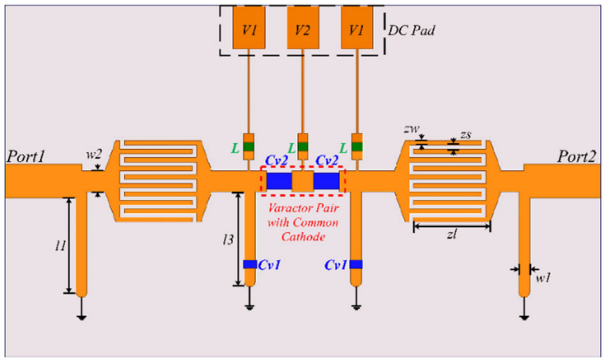

FIGURE 13. Layout of the tunable HPF.

The simulated result of the proposed tunable HPF is shown in Fig. 14. The cut-off frequency of filter can be tuned from 2.5 to 4.2 GHz. Besides, during the tuning process, the in-band return loss is greater than 11 dB, while the out-of-band suppression level is greater than 30 dB.

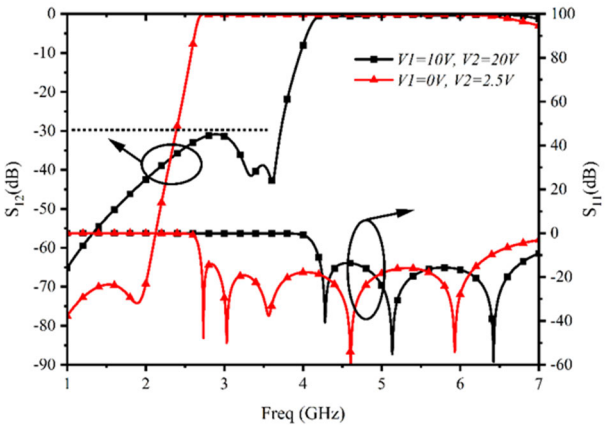

FIGURE 14. Simulated result of the tunable HPF.

E. DESIGN OF FULLY TUNABLE BPF

The fully tunable BPF can be obtained by cascading the switchable notch filter, tunable LPF and tunable HPF designed before. The layout and fabricated photograph of the tunable BPF are shown in Fig. 15, the proposed filter are fabricated on Rogers 5880 with relative dielectric constant $\varepsilon_r = 2.2$ and thickness $h = 0.508$ mm. HFSS is employed to optimize the tunable BPF, and the overall size of the BPF is 52 mm($0.69\lambda_g$) × 14 mm($0.18\lambda_g$) (λ_g represents the guided wavelength at 2.9 GHz).

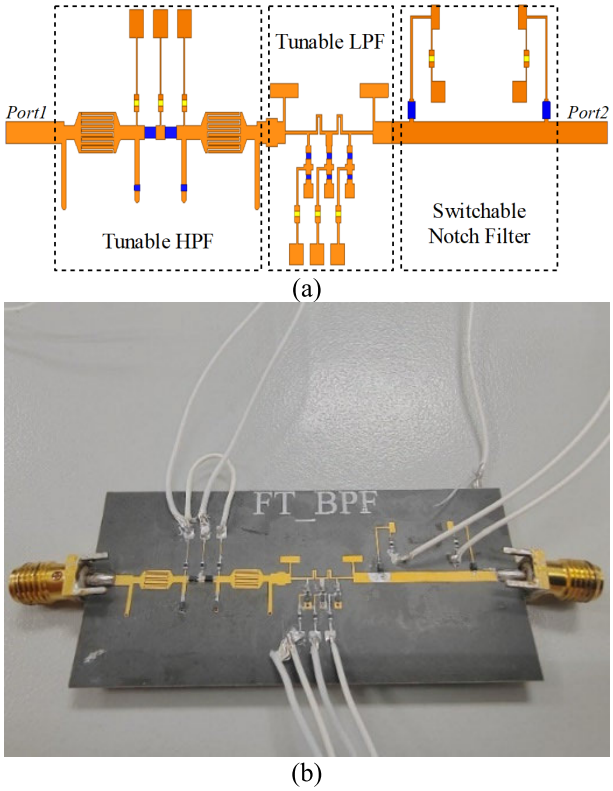

FIGURE 15. Tunable BPF (a) Layout (b) Fabricated photograph.

III. SIMULATED AND MEASURED RESULTS

The proposed fully tunable BPF is cascaded by tunable LPF, HPF and switchable notch filter.Thus, the proposed BPF demonstrates high flexibility and can operate in three states, i.e. single passband state, dual passband state and all-off state. When the PIN diodes are in OFF state, the BPF works in single passband state, and the center frequency and bandwidth of the BPF can be tuned by changing the bias voltages of the tunable LPF and HPF. As shown in Fig. 16, the bandwidth of the BPF can be tuned from 250 MHz to 2690 MHz at the center frequency of 3.8 GHz. During the whole tuning range, the in-band insertion loss varies from 1.45 dB to 3.8 dB, and the return loss of the filer is greater than 10dB, besides, the rejection level of stopband is greater than 30 dB. Due to the transmission zeros near the passband, the roll-off rate of the tunable LPF is above 71 dB/GHz during the tuning process. (roll-off rate is calculated by $(\alpha_{max}\text{-}\alpha_{min})/(f_{max}\text{-}f_{min})$, where $\alpha_{max/min}$ is the 30dB/3dB attenuation point, $f_{max/min}$ is the 30dB/3dB stopband frequency).

When the bandwidth of the BPF keeps constant at 1 GHz, the center frequency of the BPF can be tuned from 2.9 GHz

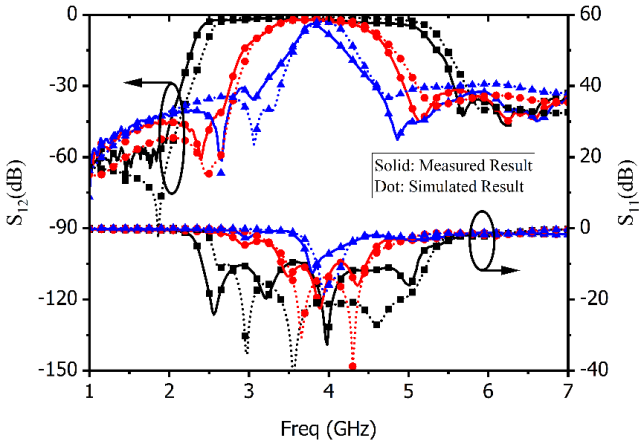

FIGURE 16. Simulated and measured frequency response.

to 4.6 GHz. Besides, the voltage reflection coefficient S_{11} is less than −10 dB and the measured insertion loss varies from 1.49 dB to 2.5 dB during the tuning process. The attenuation level of stopband is greater than 30 dB, and the roll-off rate is above 83 dB/GHz. The simulated and measured result are shown in Fig. 17.

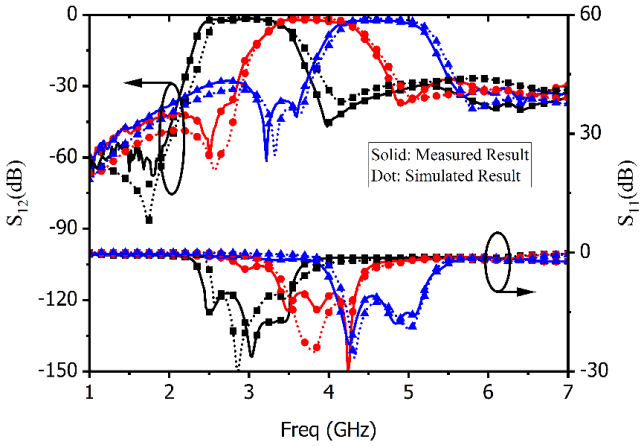

FIGURE 17. Simulated and measured frequency response.

When the PIN diode is in ON state, the notch band is enable, therefore, the BPF works in dual passband state, as shown in Fig. 18. The dual passbands work in 2.41-3.22 GHz and 4.18-5.11 GHz. And the measured in-band insertion loss of the two passband is less than 1.74 dB and 3.31 dB, respectively. Besides, the in-band return loss is greater than 12 dB, and the roll-off rate of the two passband is 94 dB/GHz and 85 dB/GHz, respectively. In dual passband state, due to the fixed center frequency of notched band, the bandwidth of the two passbands cannot be flexibly adjusted.

When the cut-off frequency of LPF is tuned to the minimum and the cut-off frequency of HPF is tuned to maximum, the BPF works in all-off state, as shown in Fig. 19. The transmission coefficient S_{12} of the filter is less than −30dB throughout the entire frequency band.

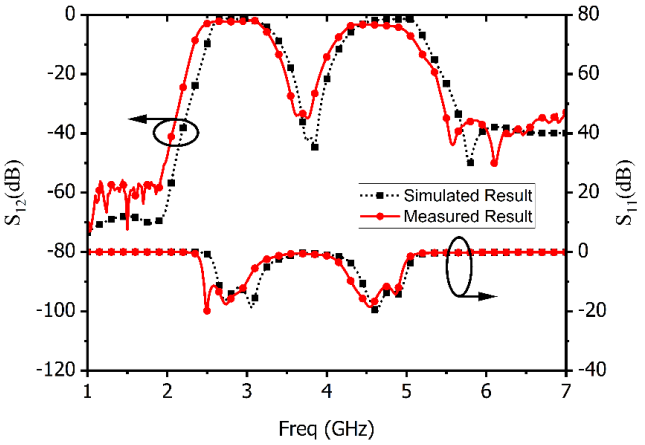

FIGURE 18. Frequency response in dual passband state.

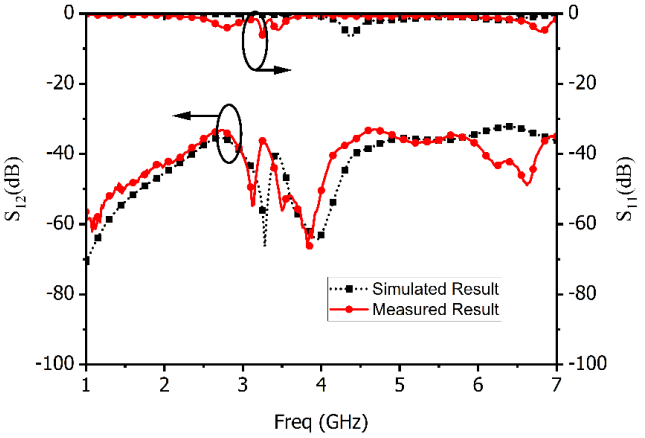

FIGURE 19. Frequency response in all-off state.

As key components in the RF front-end, the non-linearity of filters has important effect on the non-spurious dynamic range of the RF system. For tunable filters based on varactor diodes, the non-linearity is mainly affected by the varactor diodes, so it is necessary to measure the non-linearity performance of the tunable filters. The input third-order intercept point (IIP3) of the filter is measured using two-tone signal spaced by 2 MHz for the nonlinear characterization.

The measurement setup of IIP3 is shown in Fig. 20. Two-tone signal is generated by power divider with equal power ratio and phase. The input signal amplitude of tunable filters can be controlled by the variable gain amplifier (VGA). And the output IM3 and fundamental signal can be measured by signal analyzer.

The amplitude of fundamental signal and IM3 signal versus the input power is shown in Fig. 21. Because the input signal is weak, the amplitude of fundamental signal and IM3 signal increases linearly with the input power. When the amplitude of the fundamental signal is equal to that of the IM3 signal, the input signal is IIP3.

IIP3 of the tunable BPF is measured according to the measurement setup before. In single passband state, when

TABLE 1. Typical performance comparisons with prior works.

REF.	Freq(GHz)	Bandwidth (GHz)	IL (dB)	Return Loss(dB)	Rejection Level(dB)	Switchable Single/dual Band	All-off State	NoCV	NoLC	Size(λg×λg)
[4]	2.5-3	0.63-1.5	1.1	>10	10	NO	NO	4	2	NG
[8]	1.7-2.7	0.05-0.11	4.9	>10	26	NO	NO	2	5	0.12×0.41
[14]	0.4-0.53	0.008-0.014	2	>10	60	NO	NO	2	NG	0.04×0.24
[18]	0.8-1.95	0.18-1.39	5.2	>11.5	20	NO	NO	5	6	0.1×0.3
[19]	10.2-15.7	5.5-11.5	3.9	>10	25	NO	YES	7	2	0.74×2.2
Proposed	2.9-4.6	0.25-2.69	3.8	>10	30	YES	YES	5	3	0.18×0.69

Note: NoCV: number of control voltages; NoLC: number of lumped capacitors; NG: not given.

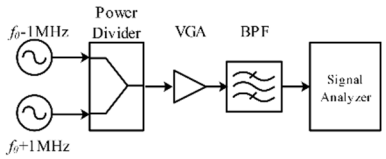

FIGURE 20. The IIP3 measurement setup.

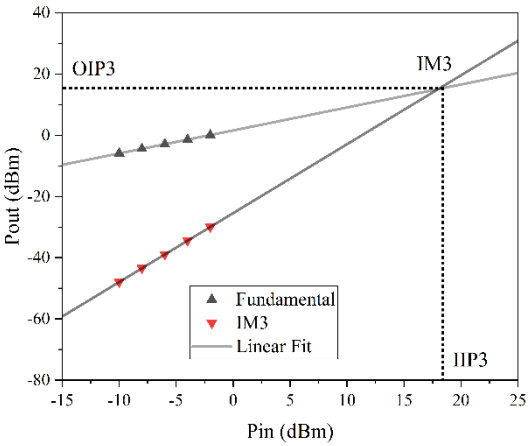

FIGURE 21. The fundamental and IM3 signal.

the bandwidth of the BPF is tunable, the IIP3 varies from 14.7 dBm to 23.6 dBm. And when the center frequency of the BPF is tunable, the measured IIP3 varies from 13.9 dBm to 22.3 dBm. In dual passband state, the measured IIP3 of the two passband is less than 18.4 dBm and 17.1 dBm, respectively.

Table 1 shows the comparison between this work and other fully tunable BPFs. As shown in Table 1, the proposed fully tunable BPF shows wider bandwidth tuning range than other works. Besides, the proposed filter also realize better stopband rejection level performance. More importantly, the proposed fully tunable BPF is capable of operating in single passband state, dual passband state and all off state, demonstrating high flexibility. However, the proposed fully tunable BPF requires five control voltages that may introduce cumbersome inconveniences in applications. How to reduce the number of control voltages may be a potential research issue for fully tunable filters based on cascade schemes.

IV. CONCLUSION

A fully tunable bandpass filter with wide bandwidth tuning range and switchable single/dual band is proposed in this paper. The fully tunable BPF is realized by cascading a tunable LPF, a tunable HPF and a switchable notch filter directly. By controlling the cut-off frequency of the tunable LPF and HPF, the center frequency and bandwidth can be tuned, and bandwidth tuning range with 0.25-2.69 GHz (10.8:1) is realized. Besides, the proposed BPF can realize reconfigurable passband, i.e. single passband state, dual passband state and all-off state, and the high flexibility makes the proposed BPF very attractive in carrier aggregation scenarios.

REFERENCES

[1] E. Doumanis, G. Goussetis, J. Vuorio, K. Hautio, O. Amper, E. Kuusmik, and J. Pallonen, "Tunable filters for agile 5G new radio base transceiver stations," *IEEE Microw. Mag.*, vol. 22, no. 11, pp. 26–37, Nov. 2021.

[2] A. C. Guyette, "Intrinsically switched varactor-tuned filters and filter banks," *IEEE Trans. Microw. Theory Techn.*, vol. 60, no. 4, pp. 1044–1056, Apr. 2012.

[3] H. Islam, S. Das, T. Bose, and T. Ali, "Diode based reconfigurable microwave filters for cognitive radio applications: A review," *IEEE Access*, vol. 8, pp. 185429–185444, 2020.

[4] Z.-H. Chen and Q.-X. Chu, "Wideband fully tunable bandpass filter based on flexibly multi-mode tuning," *IEEE Microw. Wireless Compon. Lett.*, vol. 26, no. 10, pp. 789–791, Oct. 2016.

[5] B. Lan, J. Xu, C. Guo, and J. Ding, "A fully tunable bandpass filter using a varactor-tuned short-stub loaded resonator," in *Proc. Int. Conf. Microw. Millim. Wave Technol. (ICMMT)*, Chengdu, China, May 2018, pp. 1–3.

[6] C. Teng, P. Cheong, S.-K. Ho, K.-W. Tam, and W.-W. Choi, "Design of wideband bandpass filter with simultaneous bandwidth and notch tuning based on dual cross-shaped resonator," *IEEE Access*, vol. 8, pp. 27038–27046, 2020.

[7] M. R. A. Nasser, R. K. Jaiswal, and D. Psychogiou, "A compact bandpass filter manifold with ultrawide frequency and bandwidth tuning," *IEEE Access*, vol. 11, pp. 41054–41060, 2023.

[8] P.-L. Chi, T. Yang, and T.-Y. Tsai, "A fully tunable two-pole bandpass filter," *IEEE Microw. Wireless Compon. Lett.*, vol. 25, no. 5, pp. 292–294, May 2015.

[9] G. Zhang, Y. Xu, and X. Wang, "Compact tunable bandpass filter with wide tuning range of centre frequency and bandwidth using short coupled lines," *IEEE Access*, vol. 6, pp. 2962–2969, 2018.

[10] A. Kumar and N. P. Pathak, "Varactor-incorporated bandpass filter with reconfigurable frequency and bandwidth," *Microw. Opt. Technol. Lett.*, vol. 59, no. 8, pp. 2083–2089, Aug. 2017.
[11] C.-F. Chen, G.-Y. Wang, and J.-J. Li, "Microstrip switchable and fully tunable bandpass filter with continuous frequency tuning range," *IEEE Microw. Wireless Compon. Lett.*, vol. 28, no. 6, pp. 500–502, Jun. 2018.
[12] B. Lan, C. Guo, and J. Ding, "A fully tunable two-pole bandpass filter with wide tuning range based on half mode substrate integrated waveguide," *Microw. Opt. Technol. Lett.*, vol. 60, no. 4, pp. 865–870, Apr. 2018.
[13] J. Guo, B. You, and G. Q. Luo, "A miniaturized eighth-mode substrate-integrated waveguide filter with both tunable center frequency and bandwidth," *IEEE Microw. Wireless Compon. Lett.*, vol. 29, no. 7, pp. 450–452, Jul. 2019.
[14] Z. Zhang, F. Zhao, and A. Wu, "A tunable open ring coupling structure and its application in fully tunable bandpass filter," *Int. J. Microw. Wireless Technol.*, vol. 11, no. 8, pp. 782–786, Oct. 2019.
[15] M. Fu, Q. Feng, Q. Xiang, and N. Jiang, "Fully tunable filter with cross coupling and reconfigurable transmission zero," *Int. J. RF Microw. Comput.-Aided Eng.*, vol. 30, no. 12, pp. 1–10, Dec. 2020.
[16] C.-F. Chen, "Design of a microstrip three-state switchable and fully tunable bandpass filter with an extra-wide frequency tuning range," *IEEE Access*, vol. 8, pp. 66438–66447, 2020.
[17] K. Song, M. Fan, and Y. Fan, "Novel reconfigurable bandpass filter with wide tunable bandwidth," in *IEEE MTT-S Int. Microw. Symp. Dig.*, Guangzhou, China, May 2019, pp. 1–3.
[18] M. Fan, K. Song, and Y. Fan, "Reconfigurable bandpass filter with wide-range bandwidth and frequency control," *IEEE Trans. Circuits Syst. II, Exp. Briefs*, vol. 68, no. 6, pp. 1758–1762, Jun. 2021.
[19] Z. Wei, T. Yang, P.-L. Chi, X. Zhang, and R. Xu, "A 10.23–15.7-GHz varactor-tuned microstrip bandpass filter with highly flexible reconfigurability," *IEEE Trans. Microw. Theory Techn.*, vol. 69, no. 10, pp. 4499–4509, Oct. 2021.
[20] A. I. Zverev, *Handbook of Filter Synthesis*. Hoboken, NJ, USA: Wiley, 1967.
[21] J.-S. Hong and M. J. Lancaster, *Microstrip Filters for RF/Microwave Applications*. Hoboken, NJ, USA: Wiley, 2001.

SHUANG LI was born in 1990. He received the B.S. and M.S. degrees from Xidian University, China, in 2013 and 2016, respectively. He is currently pursuing the Ph.D. degree with China Academy of Space Technology (Xi'an). His research interest includes tunable and reconfigurable microwave components.

SHENGXIAN LI was born in 1974. He received the M.S. degree from China Academy of Space Technology (Xi'an), China, in 1999. He is currently a Research Fellow with China Academy of Space Technology (Xi'an). His research interests include microwave passive technology and satellite communication.

JIANRONG YUAN was born in 1980. He received the B.S. degree from Chongqing University, China, in 2002, and the M.S. degree from China Academy of Space Technology (Xi'an), China, in 2005. His research interest includes microwave passive technology.

JUN LIU was born in 1988. He received the M.S. degree from China Academy of Space Technology (Xi'an), China, in 2014. His research interest includes microwave filter technology.

MAN SHI was born in 1998. She received the M.S. degree from China Academy of Space Technology (Xi'an), China, in 2023. Her research interest includes tunable microwave filter technology.